

The Bridged Lamellar Structure of Synthetic Waxes Determined by Electron Crystallographic Analysis

Douglas L. Dorset

Electron Crystallography Laboratory, Hauptman-Woodward Institute, 73 High Street, Buffalo, New York 14203-1196

Received: December 13, 1999

Single-crystal structures of two synthetic waxes were solved in projection from electron diffraction data to show that the bridged lamellar model for low molecular weight linear polyethylenes is again expressed. Shell “Callista 158” often crystallizes to mimic $n\text{-C}_{35}\text{H}_{72}$ with an average lamellar spacing of $c/2 = 47.2 \text{ \AA}$. Sasol “Parafint” wax can crystallize to resemble $n\text{-C}_{63}\text{H}_{128}$ with an average lamellar spacing of $c/2 = 82.0 \text{ \AA}$. Both materials pack in space group $A2_1am$ with $a \approx 7.42$, $b \approx 4.96 \text{ \AA}$. No evidence is found for extensive methyl branch inclusion in the lamellae and the sharp $0kl$ diffraction patterns extend to 1.1 \AA (or higher) resolution. Crystal structure models agree well with observed diffraction amplitudes ($R = 0.23$ in both cases).

Introduction

In addition to producing automobile fuels from water gas ($\text{CO} + \text{H}_2$), the Fischer–Tropsch synthesis is an important source of paraffin waxes, as reviewed recently in an historical perspective.¹ This catalyst-facilitated synthesis has been extensively studied in terms of reaction mechanism^{1,2} and the nature of the final products.³ The amount of chain branching in the paraffin components in the wax apparently depends on the type of catalyst used.² Infrared spectroscopic⁴ and X-ray diffraction⁵ studies have demonstrated that the waxes have a crystalline nature, but nuclear magnetic resonance spectroscopy⁶ also indicates flexible chain moieties in the solid, not entirely explained by a trapped oil fraction. A four-domain model has been proposed⁶ for the solid waxes including: the most crystalline polymethylene regions, a modification of the former region but with included methyl branches, a disordered lamellar interface and finally, an ill-defined region with small molecular weight paraffinic molecules. Although the polymethylene chain packing (identical to the unit cell of polyethylene⁷) is often emphasized, the existence of an average lamellar structure has been established for some fractions.³ This model has also been suggested⁸ to be appropriate for natural waxes.

Uncertainties inherent in interpreting the powder diffractometry of bulk polymethylene chain samples have been clarified recently in the study of individual oriented microcrystals by electron crystallography.⁹ Single-crystal structures of refined paraffin waxes¹⁰ have shown them to possess a well-developed lamellar structure so that, on average, they are difficult to distinguish from the binary n -paraffin solid solutions.¹¹ A second type of solid solution crystal structure has been described more recently for low molecular weight linear polyethylenes,¹² where nascent lamellae are prevented from complete separation by long “bridging” molecules. The highly methyl-branched paraffin components in petroleum microcrystalline waxes also have been found to crystallize as bridged lamellae,¹³ although the disorder resulting from the incorporation of the methyl branches within the lamellar interface causes other discernible changes to the diffraction pattern.

There have been no similar studies of synthetic waxes. In the following description, the single-crystal structures of

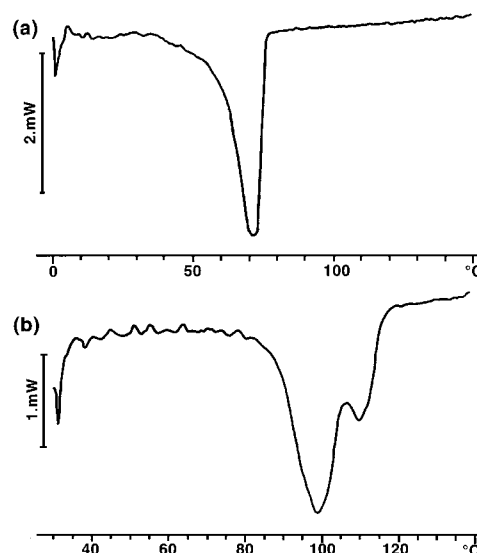


Figure 1. DSC scans for synthetic waxes. (a) Shell “Callista 158”. (b) Sasol “Parafint”.

Fischer–Tropsch waxes, based on electron crystallography, will be shown to be very similar to those of unfolded polyethylene lamellae.

Material and Methods

Waxes and Their Crystallization. Two synthetic waxes were investigated in this study, representing major industrial efforts discussed in ref 1. A sample of the Shell “Callista 158” (SC158) (Shell Chemical Company, Houston, Texas) was provided by Prof. Eberhard Bodenschatz, Department of Physics, Cornell University, Ithaca, NY. From a DSC scan (Mettler TA-3300), indicated in Figure 1a, its peak melting point is 70.9°C . In a Shell company data sheet (sent to Prof. Bodenschatz), the chain distribution is described as including C17–C63 carbon chains with a peak value at C33. From characteristic wide-angle X-ray diffraction peaks, the chains are found to pack in the orthorhombic methylene subcell. A sample of “Parafint” Fischer–Tropsch wax (PFT), produced by Sasol in South Africa was

provided by Moore and Munger Marketing, Inc. (Shelton, CT), who distribute this wax in the US. DSC measurements (Figure 1b) indicate that the wax is somewhat fractionated with a major peak melting position at 98.6 °C and a higher temperature endotherm at 109.6 °C. Although no specific chain length data have been provided by the supplier, there is evidence (see below) that this material is similar to the "superhard" Sasol Fischer-Tropsch fraction examined originally by Le Roux² with a mean carbon chain length of C68.

Initially, these waxes were taken up in a dilute solution with light petroleum (heated if necessary to solubilize the material) and thin lamellar microcrystals were formed by evaporation onto a carbon-film-covered 300 mesh copper electron microscope grid. Following earlier procedures,¹⁴ epitaxially oriented samples were obtained by first evaporating the dilute light petroleum solution onto a freshly cleaved mica sheet to form a thin organic film. With carbon covered electron microscope grids placed face down onto the organic film, an excess of benzoic acid crystals was distributed over this surface and a sandwich completed by adding the other half of the cleaved mica sheet. Using a thermal gradient the organic solid was first co-melted and then recrystallized to orient the linear chain compounds on the diluent crystal surface, as described by a binary eutectic phase diagram.¹⁵ The physical sandwich could then be separated mechanically and the benzoic acid removed by sublimation overnight in a vacuum coating unit to permit investigation of the oriented wax crystals.

Often the epitaxial orientation achieved by rapid growth is insufficient for crystallographic studies in the electron microscope. As shown earlier with natural waxes¹⁶ or low molecular weight linear polyethylene,¹² the sample crystallinity could be improved by annealing the linear chain materials (Mettler FP82 heating stage controlled by a FP90 control unit) in the presence of the benzoic acid substrate at a temperature within the onset of the melting endotherm for 4.5 h. The annealing experiment was not necessary for the SC158 material. The Sasol PFT, on the other hand, was annealed at 80 °C because, otherwise, the initial crystallization often did not show any evidence of lamellar order. The benzoic acid was then removed by sublimation in vacuo after the material had been cooled back to room temperature.

Diffraction Experiments. Electron diffraction experiments were carried out at 100 kV with a JEOL JEM-100CX II electron microscope, taking usual precautions to minimize radiation damage to the thin organic crystals,⁹ i.e., use of a small beam current density, a short exposure time, and recording the diffraction patterns on X-ray film (Kodak DEF-5 or CEA Reflex). The selected area most frequently employed sampled a 2.9 μm diameter of the specimen (calibrated by a carbon diffraction replica). All measurements were made at room temperature. Diffraction spacings on electron diffraction patterns were calibrated against an Au^o powder standard.

Intensity data were measured on the experimental diffraction films with a Joyce-Loebl Mk. IIIC flat-bed microdensitometer, using a triangular fit to the peak profile. Care was taken to establish that the intensity data were internally consistent, as established by suitably low values of R_{merge} when two equivalent patterns were compared or R_{sym} when symmetry equivalent reflections in a single pattern were compared.¹⁷ Because the thin organic crystals were plastically deformed, there was no need to apply a Lorentz correction to the intensity data.⁹

Structure Analysis. As is typical for electron diffraction patterns from epitaxially oriented orthorhombic polymethylene assemblies (see Figure 2), there are two parts of the $0kl$ patterns which immediately give a qualitative overview of the chain

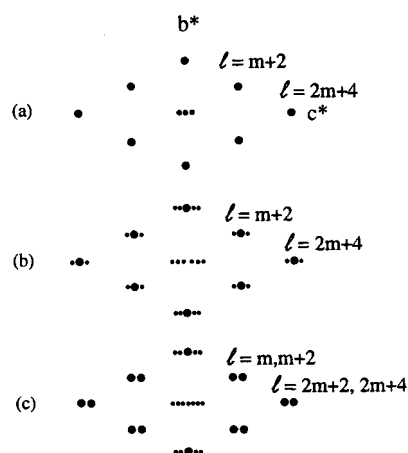


Figure 2. Schematic $0kl$ electron diffraction patterns from epitaxially oriented linear chain assemblies. (a) Only initial formation of lamellar order. Chains are mostly packed in a "nematocrystalline" array. (b) Nascent lamellar order but with appreciable bridging of interlamellar gaps by chain segments. (c) Well-separated lamellae with no bridging molecules. In each example the indices l of intense wide-angle reflections are related to the average carbon number m ($\text{C}_m\text{H}_{2m+2}$) of the lamella.

packing. At low angle, the $00l$ reflections measure the average lamellar thickness. The intense wide angle $01l$ and $00l$ reflections are due to the methylene chain packing. If these reflections are not split into two intense peaks, as also found for low molecular weight linear polyethylene, then the lamellar separation is incomplete. Indices of the strong $0kl$ reflections, moreover, are simply related to the average carbon number of the (nascent) lamellar repeat as if it were a pure n -paraffin (Figure 2). From the indices of these reflections, by consulting parent orthorhombic n -alkane crystal structures, the space group can be determined to be either $A2_1am$ for the odd-chainlike structures and $Pca2_1$ for the even-chainlike structures.¹⁸ Poly-disperse assemblies of linear chains can crystallize in neighboring microareas in either orthorhombic unit cell, so that several average local structures can exist for a given material.¹⁸

Crystallographic direct phasing methods have been used to determine structures of n -paraffins and their solid solutions in this $[100]$ projection.¹⁹ For these materials only the $00l$ structure factor magnitudes were used initially to calculate a one-dimensional Fourier transform to represent the lamellar profile. Algebraic phase values were assigned to reflections within two intensity envelopes (low and wide angle), where approximate centrosymmetry was assumed. For a "reasonable" one-dimensional lamellar profile with carbon peak positions and suggested occupancy factors, the z/c coordinates of these atoms were obtained. For both waxes, completing the two-dimensional model required adding y/b carbon positions typical of the orthorhombic B-polymorph odd-chain alkanes²⁰ in $A2_1am$, i.e., y/b are 0.190 and 0.309 for odd- and even-numbered carbon positions. Here $a \approx 7.42$, $b \approx 4.96$ Å. These carbon coordinates were then used to calculate the amplitudes of the complete $0kl$ pattern, the fit measured by the crystallographic residual ($R = \sum ||F_{\text{obs}}| - k|F_{\text{calcd}}|| / \sum ||F_{\text{obs}}||$). The entire sequence of carbon positions obtained from the one-dimensional Fourier transform was regarded as a rigid diffraction grating that could not be varied. Because of the relative paucity of data collected, only an atomic occupancy profile and an overall isotropic temperature factor were permitted as variable parameters, if necessary, so that the R value figure of merit might retain some statistical significance.²¹

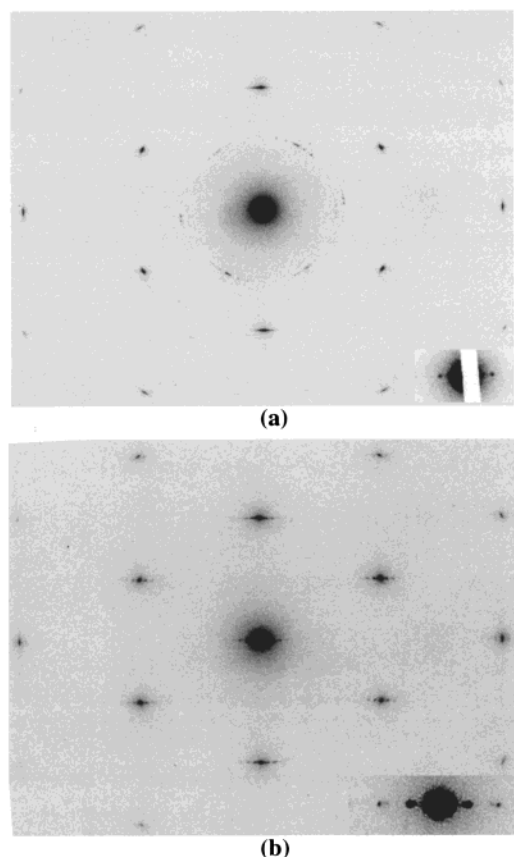


Figure 3. Electron diffraction patterns from oriented synthetic waxes. (a) "Parafint" (inset: lamellar reflections) (b) "Callista 158" (inset: lamellar reflections).

TABLE 1: Observed and Calculated Structure Factor Amplitudes for Sasol "Parafint" Wax

$0kl$	$ F_{\text{obs}} $	$ F_{\text{calcd}} $	phase ^a
00 2	0.66	0.58	π
00 4	0.34	0.57	π
00 130	1.55	0.97	π
01 65	1.84	1.49	$\pi/2$
02 0	3.04	3.48	π
02 130	0.73	0.46	0
03 65	1.22	1.22	$-\pi/2$

^a Nearly approximate centrosymmetric value.

Results

A representative $0kl$ electron diffraction pattern from the heavier Sasol PFT wax is shown in Figure 3a. The parent polyethylene-like diffraction pattern accounts for the most intense wide-angle reflections which remain as unsplit singlet diffraction peaks. Separate lamellar $00l$ reflections (at most two orders) are observed. Indices of the $01l$ reflection according to the rules given in Figure 2a establish that a distribution of crystal structures can be found mimicking paraffins with chain lengths in the C60 to C68 range, thus approximately matching the cited mean literature value.³

An intensity data set from a typical C63-like structure was assembled by averaging over several diffraction patterns. The average lamellar spacing is $c/2 = 82.0 \pm 3.3$ Å, compared to a predicted²² value of 82.1 Å for $n\text{-C}_{63}\text{H}_{128}$. After constructing a lamellar model, aided by the one-dimensional Fourier transform of the $00l$ reflections (with all phase values assumed to be near π radians), a structure factor calculation (Table 1) produced a reasonable match ($R = 0.23$) to the observed amplitudes, particularly if a nonunitary occupancy was given to the two

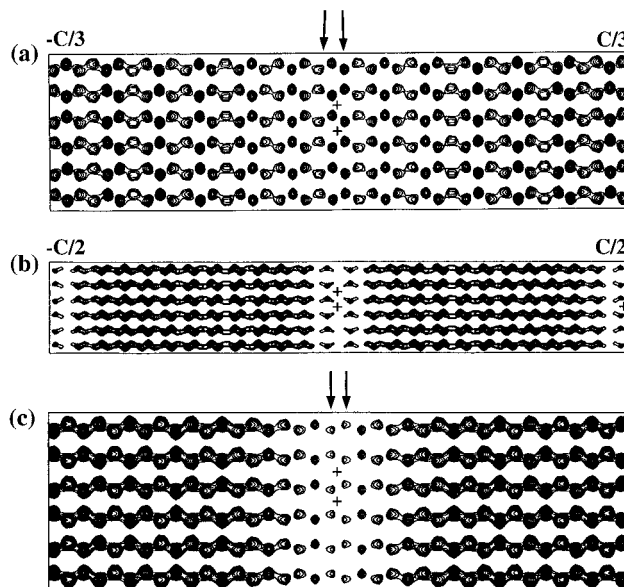


Figure 4. Electrostatic potential maps for synthetic waxes after assignment of crystallographic phase models. (a) Sasol "Parafint": enlarged detail of lamellar interface revealing bridging methylene groups (arrows) not included in the structure factor calculation. (b) Shell "Callista 158": overview of lamellar packing. (c) Shell "Callista 158": enlarged detail of lamellar interface, again revealing bridging methylene units (arrows).

outer carbon chain positions. The electrostatic potential maps calculated from observed amplitudes and experimental phases always placed carbon atom positions (arrows in Figure 4a) in the interlamellar gap, even though they had not been considered in the packing model.

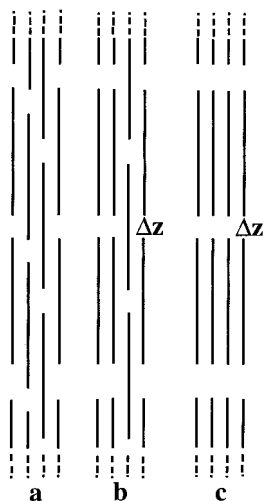
A representative pattern from the Shell "Callista 158" wax is shown in Figure 3b. Again there is a distribution of different local crystal structures betrayed by the reflection indices. The corresponding lamellar layers encompass average carbon chain numbers clustered between C34 to C36. This again approximates the peak value given above. Although there are more reflections observed in this $0kl$ pattern than for the PFT wax, the strong peak positions occur for only individual reflections as schematized in Figure 2b rather than the doublets found in patterns from the refined petroleum linear chain waxes. Collection of a data set from a representative C35-like structure assembled average intensity values obtained from numerous individual electron diffraction patterns. The average lamellar spacing was found to be $c/2 = 47.25 \pm 0.23$ Å, compared to a predicted²² value of 46.43 Å for $n\text{-C}_{35}\text{H}_{72}$. The odd-chain paraffin model again accounted well ($R = 0.23$) for the observed amplitudes (Table 2), particularly if a ramp of fractional occupancies for the six terminal carbon positions at each lamellar boundary, indicated by the one-dimensional Fourier transform of the $00l$ reflections, were included. Again, electrostatic potential maps, calculated from measured amplitudes and model phases, imposed carbon positions within the lamellar gap, even though they had not been used in the model (Figure 4b,c).

Discussion

From the crystal structure analyses of synthetic paraffin waxes, it is clear that the bridged lamellar packing found for low molecular weight linear polyethylene is again expressed. The sequence of structures possible for oriented chain assemblies is shown in Figure 5. As also found with very long chain n -paraffins,²³ an initial "nematocrystalline" array with little or no lamellar order can be driven by annealing to form a

TABLE 2: Observed and Calculated Structure Factor Amplitudes for Shell “Callista 158” Wax

$0k\ l$	$ F_{\text{obs}} $	$ F_{\text{calcd}} $	phase ^a
00 2	1.36	1.60	π
00 4	0.91	1.16	π
00 6	0.46	0.70	π
00 72	0.18	0.28	0
00 74	1.64	1.58	π
00 76	0.19	0.20	0
01 33	0.26	0.21	$\pi/2$
01 35	0.44	0.29	$\pi/2$
01 37	2.18	1.79	$-\pi/2$
01 39	0.44	0.44	$\pi/2$
01 41	0.25	0.18	$\pi/2$
02 0	4.21	4.01	π
02 2	0.24	0.60	0
02 4	0.16	0.44	0
02 6	0.12	0.26	0
02 72	0.12	0.14	π
02 74	0.79	0.83	0
02 76	0.15	0.11	π
03 35	0.16	0.29	$-\pi/2$
03 37	1.31	1.79	$\pi/2$
03 39	0.16	0.24	$-\pi/2$
04 0	0.22	0.11	0

^a Nearly approximate centrosymmetric value.**Figure 5.** Schema of molecular packing for linear chains (represented by straight lines), compare to Figure 2. (a) Nematocrystalline array: nascent or no lamellar order. (b) Incomplete lamellar separation where some bridging chains constrain Δz , the interlamellar gap spacing, to $3c_s/2$ where $c_s/2$ is the chain methylene repeat. (c) Stable lamellar separation (no bridging chains) where $\Delta z \neq 3c_s/2$.

completely separated lamellar array via intermediate assemblies where nascent lamellae still include some long chain bridging the interfacial gap. Diffraction patterns from the SC158 sample strongly resemble those from the low molecular weight linear polyethylene¹² in that numerous sharp reflections are observed to very high resolution. (In fact the average carbon number of the lamellar repeat for the polyethylene, C41, is not greatly different from the average found for the synthetic wax.) Although the “Parafint” structure, with the longer average chain packing, is somewhat less ordered (evidenced by the absence of satellite reflections near the strong polyethylene peaks), diffraction is still observed to 1.1 Å resolution.

From the appearance of the diffraction patterns, it is clear also that the major chain component of either wax is mostly linear, i.e., with a low concentration of branches. For the Sasol ‘superhard’ Fischer–Tropsch wax examined by Le Roux,⁴ the average number of methyl branches is 0.41 per 100 chain

carbons. A recent electron crystallographic study¹³ of highly branched waxes and methyl-branched *n*-paraffins reveals that, although the rectangular layer structure is retained for the nascent lamellar packing, the incorporation of methyl branches leads to disorder observed as a characteristic broadening of the strong 011 reflection, not observed in patterns from the synthetic waxes.

Accumulated electron crystallographic experience with single crystals of real wax samples^{10–13} indicates, therefore, that there are two archetypical structures for linear chain assemblies. If there is a narrow Gaussian distribution of chain components,²⁴ as in the refined waxes, then the lamellar order can be well-expressed with average flat end plane surfaces.¹⁰ Broader distributions, particularly if they involve longer chain fractions, will lead to bridged lamellar structures.^{12,13} Chromatographic studies of the Fischer–Tropsch waxes,²⁵ in fact, indicate the presence of such longer components as a higher molecular weight “tail”, just as there are residual longer chain fractions in the polyethylenes,²⁶ despite a low polydispersity index. Similar behavior is found for certain natural products such as carnauba and bee honeycomb waxes, where longer chain components, e.g., fatty acid esters of long chain diols, have been described.²⁷ Inclusion of methyl branches is a variant of the bridged lamellar structure but the interpenetrations are not as extensive as for chain-extended polyethylene or these synthetic waxes.¹³

How do these accumulated results match the model once proposed⁶ for the Fischer–Tropsch and natural waxes? Obviously the nascent lamellar order is a given, even though the possibility of nematocrystalline disorder must be also considered for samples rapidly cooled from the melt (e.g., the “Parafint”). The inclusion of methyl branches in the most crystalline polymethylene packing region is not energetically allowed and will occur at interfaces only if gaps are left to accommodate the branches in adjacent chain segments. The major, yet-unanswered, question seems to be the role of the lower molecular weight “oil” component, thought to be included also within the lamellar interface. There is no definitive answer to this question from electron crystallography, even though the high-vacuum conditions of the experiment might distill away this fraction and trigger a recrystallization process.

Acknowledgment. Research was funded by a grant from the National Science Foundation (CHE-9730317), which is gratefully acknowledged. Thanks are due also to Prof. Eberhard Bodenschatz and to Moore & Munger Marketing, Inc., for providing the materials used in this study.

References and Notes

- (1) Schulz, H. *Appl. Catal.* **1999**, A186, 3.
- (2) Le Roux, J. H.; Dry, L. J. *J. Appl. Chem. Biotechnol.* **1972**, 22, 719.
- (3) Le Roux, J. H. *J. Appl. Chem.* **1970**, 20, 203.
- (4) Le Roux, J. H. *J. Appl. Chem.* **1969**, 19, 86.
- (5) Retief, J. J.; Le Roux, J. H. *South Afr. J. Sci.* **1983**, 79, 234.
- (6) Le Roux, J. H.; Loubser, N. H. *South Afr. J. Sci.* **1980**, 76, 157.
- (7) Lourens, J. A. J.; Reynhardt, E. C. *J. Phys. D: Appl. Phys.* **1979**, 12, 1963.
- (8) Basson, I.; Reynhardt, E. C. *Chem. Phys. Lett.* **1992**, 198, 367.
- (9) Abrahamsson, S.; Dahlen, B.; Löfgren, H.; Pascher, I. *Prog. Chem. Fats Other Lipids* **1978**, 16, 125.
- (10) Basson, I.; Reynhardt, E. C. *J. Phys. D: Appl. Phys.* **1988**, 21, 1421, 1429, 1434.
- (11) Dorset, D. L. *Structural Electron Crystallography*; Plenum: NY, 1995.
- (12) Dorset, D. L. *Acta Crystallogr.* **1995**, B51, 1021. Dorset, D. L. *J. Phys. D: Appl. Phys.* **1997**, 30, 451. Dorset, D. L. *Z. Kristallogr.* **1999**, 214, 362.
- (13) Dorset, D. L. *Z. Kristallogr.* **1999**, 214, 229.
- (14) Dorset, D. L. *Macromolecules* **1999**, 32, 162.

- (13) Dorset, D. L. *Energy Fuels*. In press.
- (14) Wittmann, J. C.; Hodge, A. L.; Lotz, B. *J. Polym. Sci., Polym. Phys. Ed.* **1983**, *21*, 2495.
- (15) Dorset, D. L.; Hanlon, J.; Karet, G. *Macromolecules* **1989**, *22*, 2169.
- (16) Dorset, D. L. *J. Phys. D: Appl. Phys.* **1999**, *32*, 1276.
- (17) Dorset, D. L.; McCourt, M. P.; Li, G.; Voigt-Martin, I. G. *J. Appl. Crystallogr.* **1998**, *31*, 544.
- (18) Dorset, D. L. *Macromolecules* **1987**, *20*, 2782.
- (19) Dorset, D. L.; Zemlin, F. *Ultramicroscopy* **1990**, *33*, 227. Dorset, D. L. *Proc. Natl. Acad. Sci. U.S.A.* **1990**, *87*, 8541.
- (20) Dorset, D. L. *Z. Kristallogr.* **1999**, *214*, 223.
- (21) Hamilton, W. C. *Statistics in Physical Science*; Ronald, NY, 1964; pp 157ff.
- (22) Nyburg, S. C.; Potworowski, J. A. *Acta Crystallogr.* **1973**, *B29*, 347.
- (23) Zhang, W. P.; Dorset, D. L. *J. Polym. Sci. B: Polym. Phys.* **1990**, *28*, 1223.
- (24) Jayalakshmi, V.; Selvavathi, V.; Sekar, M. S.; Sawan, B. *Pet. Sci. Technol.* **1999**, *17*, 843.
- (25) Stenger, H. G.; Johnson, H. E.; Satterfield, C. N. *J. Catal.* **1984**, *86*, 477.
- (26) Prasad, A.; Mandelkern, L. *Macromolecules* **1989**, *22*, 914.
- (27) Stransky, K.; Streibl, M.; Kubelka, V. *Collect. Czech. Chem. Commun.* **1971** *36*, 2281. Warth, A. *The Chemistry and Technology of Waxes*; Reinhold: NY, 1947.